Published in final edited form as:
J Cell Mol Med. 2009 November ; 13(11-12): 4422–4431. doi:10.1111/j.1582-4934.2008.00623.x.

The α_{1H} Ca^{2+} Channel Subunit is Expressed in Mouse Jejunal Interstitial Cells of Cajal and Myocytes

Simon J. Gibbons[1,2,3,*], **Peter R Strege**[1,2,3], **Sha Lei**[1,2,3], **Jaime L Roeder**[1,2,3], **Amelia Mazzone**[1,2,3], **Yijun Ou**[1,2,3], **Adam Rich**[4], and **Gianrico Farrugia**[1,2,3]

[1] Enteric Neuroscience Program, Mayo Clinic College of Medicine, Rochester, MN, USA

[2] Department of Physiology and Biomedical Engineering, Mayo Clinic College of Medicine, Rochester, MN, USA

[3] Miles and Shirley Fiterman Center for Digestive Diseases, Mayo Clinic, Rochester, MN, USA

[4] Department of Biological Sciences, SUNY Brockport, 350 New Campus Drive, Brockport, NY 14420, USA

Abstract

T-type Ca^{2+} currents have been detected in cells from the external muscular layers of gastrointestinal smooth muscles and appear to contribute to the generation of pacemaker potentials in interstitial cells of Cajal from those tissues. However, the Ca^{2+} channel α subunit responsible for these currents has not been determined. We established that the α subunit of the α_{1H} Ca^{2+} channel is expressed in single myocytes and interstitial cells of Cajal using reverse transcription and polymerase chain reaction from whole tissue, laser capture microdissected tissue, and single cells isolated from the mouse jejunum. Whole cell voltage clamp recordings demonstrated that a nifedipine and Cd^{2+} resistant, mibefradil-sensitive current is present in myocytes dissociated from the jejunum. Electrical recordings from the circular muscle layer demonstrated that mibefradil reduced the frequency and initial rate of rise of the electrical slow wave. Gene targeted knockout of both alleles of the *cacna1h* gene, which encodes the α_{1H} Ca^{2+} channel subunit, resulted in embryonic lethality due to death of the homozygous knockouts prior to E13.5 days in utero. We conclude that a channel with the pharmacological and molecular characteristics of theα_{1H} Ca^{2+} channel subunit is expressed in interstitial cells of Cajal and myocytes from the mouse jejunum, and that ionic conductances through the α_{1H} Ca^{2+} channel contribute to the upstroke of the pacemaker potential. Furthermore, the survival of mice that do not express the α_{1H} Ca^{2+} channel protein is dependent on the genetic background and targeting approach used to generate the knockout mice.

Keywords

Gastrointestinal motility; Electrical slow wave; Ion channels; Transgenic Animals

INTRODUCTION

T-type or low voltage activated Ca^{2+} currents are detected in a variety of smooth muscle cells including gastrointestinal, vascular, myometrial and genito-urinary tract myocytes [1–4] where they are nearly always co-expressed with the L-type, high-voltage activated Ca^{2+}

*Author for correspondence: Simon J Gibbons PhD, Enteric Neuroscience Program, Mayo Clinic, Guggenheim 838, 200 First Street SW, Rochester MN 55905, Tel 507 284 4695, Fax 507 284 0266; gibbons.simon@mayo.edu.

currents. Unlike L-type Ca^{2+} currents, the physiological roles of T-type Ca^{2+} currents are not clear although several studies have implicated these currents in regulation of rhythmic oscillations of membrane potential and control of myocyte proliferation during vascular development and remodeling [2].

The presence of low voltage-activated, Ca^{2+}-permeable ionic conductances in cells from the external muscle layers of gastrointestinal smooth muscles has been reported in smooth muscle cells from the mouse colon [5], guinea pig taenia coli [6,7], rat colon [3] and human colon [4] as well as interstitial cells of Cajal (ICC) from dog colon [8] and mouse colon and small intestine [9]. Many of these studies have identified the conductance as a T-type Ca^{2+} current [3,4,6,7], and some of the other currents recorded in colonic myocytes have T-type properties [8,9]. The physiological role of T-type Ca^{2+} currents in gastrointestinal myocytes has not been determined.

Data that do not support the presence of T-type Ca^{2+} channels in myocytes come from studies showing that inward Ca^{2+} permeable conductances recorded in myocytes from mouse colon are not as selective for Ca^{2+} as expected for T-type Ca^{2+} channels or are impermeable to Ba^{2+}. These data are consistent with the presence of an unclassified non-selective cation conductance in mouse colonic myocytes [5].

Together with enteric nerves and myocytes, interstitial cells of Cajal (ICC) are required for normal gastrointestinal motility [10]. ICC generate the electrical slow wave; an oscillation in membrane potential that is required for normal phasic contractions of gastro-intestinal smooth muscles [11,12] and a role for T-type Ca^{2+} currents in the generation of slow waves has been proposed. Normal slow wave activity results from Ca^{2+} influx through plasma membrane ion channels, Ca^{2+} release from inositol 1,4,5-trisphosphate sensitive Ca^{2+} stores, and re-polarization dependent on a variety of ion channel types including non-selective cation channels and/or Ca^{2+} activated Cl^- channels [13,14]. The Ca^{2+} influx that contributes to the upstroke of the electrical slow wave is sensitive to block by agents that alter T-type Ca^{2+} channel activity. Intracellular recordings from the external muscle layers of mouse small intestine [15] indicate that a nifedipine-insensitive, Ca^{2+}-permeable conductance is responsible for Ca^{2+} influx during the electrical slow wave. In submucosal ICC from mouse colon, Ni^{2+} (10–100 μM) and mibefradil (3 μM) application resulted in a reduced rate of rise of the upstroke of the electrical slow wave [16,17]. Detailed analysis of the pacemaker potentials and electrical slow waves recorded by impaling ICC and smooth muscle cells in mouse small intestine showed that mibefradil (≥ 10 μM) reduced the rate of rise of the upstroke depolarization due to failure to entrain unitary potentials recorded from ICC [18]. Experiments using imaging of intracellular Ca^{2+} transients to follow pacemaker activity in myenteric ICC of human [19] and mouse [20] small intestine, demonstrated that the upstroke phase of the transient depends on activation of dihydropyridine-resistant Ca^{2+} influx. In mouse ileum, this Ca^{2+} influx was blocked by low concentrations of mibefradil (0.1 μM) and Ni^{2+} (100μM) [20] whereas in human small intestine [19], higher concentrations of mibefradil (10 – 50 μM) were required to inhibit the Ca^{2+} influx. These observations indicate that the conductance responsible for the upstroke of the slow wave is probably a T-type Ca^{2+} current in mouse but could be due to a different conductance in ICC of the human small intestine [21].

The genes that encode three types of T-type Ca^{2+} channels have been cloned from mouse and human tissue. These proteins, $Ca_v3.1$, $Ca_v3.2$ and $Ca_v3.3$ (or α_{1G}, α_{1H}, and α_{1I} respectively) have the properties of T-type Ca^{2+} channels in heterologous expression systems [22]. The messenger RNA (mRNA) for all three T-type Ca^{2+} channels have been identified in mouse small intestine by PCR but ICC of the deep muscular plexus (ICC-DMP) do not express any T-type Ca^{2+} channel mRNA [23]. In mouse colonic myocytes, α_{1G}

complementary DNA (cDNA) could not be amplified by reverse transcriptase polymerase chain reaction (RT-PCR) [5].

For this study we have further investigated whether T-type Ca^{2+} currents play a role in the electrical properties of the mouse jejunum based on the increased knowledge of the physiological and pharmacological properties of the T-type Ca^{2+} current. We have identified the T-type Ca^{2+} channel mRNA that is expressed in myocytes and in ICC from the external muscle layers as α_{1H} and we attempted to study the effect of knocking out expression of this gene by gene-targeted mutagenesis.

MATERIALS AND METHODS

The Institutional Animal Care and Use Committee at Mayo Clinic, Rochester approved all animal handling procedures.

Harvest of Tissue

Adult mice were killed by CO_2 inhalation followed by cervical dislocation. The small intestine was then rapidly removed and a 1–2 cm segment was rapidly frozen in liquid nitrogen to be cut into sections for laser capture microdissection. For RNA isolation, a longer 8–15 cm segment of jejunum was removed and placed in ice-cold, sterile Hanks balanced salt solution. The external muscle coat was rapidly peeled away from the mucosa and immediately placed in RNA later (Ambion, Austin, TX) for transfer to the molecular biology lab. For intracellular electrical recordings, a segment of small intestine wall, approximately 6 cm from the pylorus, was removed and placed in pre-oxygenated, normal Krebs solution at room temperature.

RNA isolation and Reverse Transcription and PCR Amplification of cDNA

RNA was isolated from the external muscle coat of the adult mouse jejunum immediately after dissection as described previously for isolation of RNA from human jejunum smooth muscle [24].

Reverse-transcription PCR (RT-PCR)

PCR amplifications were performed using GeneAmp 2400 PCR Systems (PE Biosystems, Foster City, CA) or icycler (Biorad, Hercules CA) using standard procedures as previously published [24]. Reverse transcription (RT) was performed using a mixture of random hexamer and oligo dT primers following the instructions of the manufacturer (PE Biosystems, Foster City, CA). The product of the RT reaction was then amplified for T-type Ca^{2+} channel α subunits using gene specific primers that were specifically designed to flank regions containing introns in the genomic sequence (see Table 1 for details). All PCR products were purified and sent to the Mayo Molecular Core Facility for automated DNA sequencing.

Laser Capture Microdissection (LCM)

Sections of mouse jejunum, 6 μm thick, were mounted on glass slides and fixed in ice-cold acetone according to the protocol described previously [24]. A number of spots of tissue containing about 1500 smooth muscle cells from the circular muscle layer or the longitudinal muscle layer were collected using the PIX II Cell LCM system (Arcturus Engineering Inc., Santa Clara, CA) with the 7.5 μm spot size. The caps with collected cells were then immediately placed into sterile 0.5 ml microcentrifuge tubes containing 300 μl RNA STAT-60 reagent (Tel-TEST Inc., Friendswood, TX) for isolation of total RNA. After washing with 75% ethanol, the RNA pellet was resuspended in nuclease-free water (Ambion Inc., Austin, TX) and used for the RT-PCR.

Single Cell PCR Amplification from Identified ICC

Single ICC from 3–5 day old mice were obtained as previously described [25] from a dissociation of jejunal smooth muscle that had been immunolabeled with an antibody directly conjugated to the fluorophore Alexa 546 (Invitrogen). 3–5 labeled cells and 3–5 unlabeled, spindle-shaped cells were collected using a glass pipette and placed into an RNAse free tube. A sample of bath solution was collected as a negative control against possible contamination. RNA was extracted then reverse transcribed using the ViLo Superscript III kit from Invitrogen. The cDNA was then probed for the presence of the α_{1H} Ca^{2+} channel transcript and c-Kit by two-step nested PCR using the primers shown in Table 1.

Generation of Gene Targeted Knockout Mice

Mice targeted for the knockout of the gene for the α_{1H} Ca^{2+} channel subunit by targeting the *Cacna1h* gene. The targeting vector was transfected into Lex-1 ES cells derived from 129SvEvBrd mice (Lexicon, The Woodlands TX) and the resulting clones were screened by PCR. Positively identified clones were injected into C57Bl/6 blastocysts and chimeric animals were bred to homozygosity.

Genotyping

Genotyping was done by Southern analysis using a probe (XP1) generated by PCR from genomic DNA. The genomic DNA was obtained from tails of the mice extracted using the Tissue Direct™ multiplex PCR system (GenScript, Piscataway, NJ). EcoRI was used to digest 10 μg of the genomic DNA for Southern blotting. The probe recognized a 11 kb fragment of wild-type DNA and a 9.5 kb fragment of DNA from the targeted allele.

PCR genotyping was also used to distinguish the wild-type and targeted alleles. The primers JLR5 and JLR6 were used to identify a 487 nucleotide band in the wild type alleles and primers Puro3a and KO37 identified a 520 nucleotide band in the knockout allele (see Table 1 for primer sequences).

Intracellular Electrical Recordings

The segments of small intestine were opened along the anti-mesenteric border and transferred to a Petri dish filled with fresh oxygenated normal Krebs solution. The mucosa was removed under direct vision by using a binocular microscope and muscle strips (5 × 8 mm) were cut with the long axis parallel to the longitudinal muscle layer. Muscle strips were placed in a recording chamber and pinned with the serosal side down to a Sylgard-coatedfloor. The recording chamber had a volume of 1 ml and was perfused continuously with oxygenized normal Krebs solution at 37°C at a rate of 2 ml/min. The composition of the solution was (in mM) 137.4 Na^+, 5.9 K^+, 2.5 Ca^{2+}, 1.2 Mg^{2+}, 124 Cl^-, 15.5 HCO_3^-, 1.2 $H_2PO_4^-$, and 11.5 glucose. It was continuously bubbled with 97% O_2, 3% CO_2, and maintained at pH 7.4.

Sharp glass microelectrodes filled with 3 M KCl (with input resistances ranging from 40–70 MΩ) were used to record intracellularly the membrane potential of smooth muscle cells. Approximately 30 min before recording, 1 μM nifedipine was added to reduce contractile activity of the muscle strip thereby facilitating long-term recordings from single cells. Recorded signals were amplified through an amplifier (Intra 767, WPI), digitized (Digidata 1322A, Axon Instruments), analyzed, and stored in a computer. When spontaneous electrical slow waves occurred, the membrane potential recorded between slow waves was considered the resting membrane potential (RMP). The time constant was measured as the time from the point at which the slow wave started to rise to the point the membrane potential reaches 63% of the maximum amplitude of the slow wave cycle. Values are reported as mean ± standard error (SEM). The student t-test was used to compare mean slow wave frequency in

control conditions and during drug treatment. A P value ≤ 0.05 was considered a significant difference.

Whole Cell Voltage Clamp Recordings

Currents were recorded from voltage clamped cells at 22 °C using standard whole cell techniques [26,27]. Microelectrodes were pulled from Kimble KG-12 glass on a P-97 puller (Sutter Instruments, Novato, CA). Electrodes coated with R6101 (Dow Corning, Midland, MI) were fire-polished to a final resistance of 3 to 5 MΩ. Currents were amplified, digitized, and processed using an Axopatch 200B amplifier, Digidata 1322A, and pCLAMP 9.2 software (Axon Instruments). Whole cell records were sampled at 10 kHz and filtered at 4 kHz with an 8 pole Bessel filter. During analysis, the 0.1 ms (10 Hz) sampling interval of whole cell records was decimated 10-fold down to 1 ms (1 kHz). 70–85% series resistance compensation with a lag of 60 μs was applied during each recording. Freshly dissociated mouse intestinal smooth cells were held at a potential of −100 mV and stepped from −80 to 35 mV in 5 mV intervals for 400 ms. The start-to-start time was 516 ms.

Drug and solutions

The intracellular solution contained (in mM) 130 Cs^+, 125 methanesulfonate, 20 Cl^-, 5 Na^+, 5 Mg^{2+}, 5 HEPES, 2 EGTA, 2.5 ATP, and 0.1 GTP, equilibrated to pH 7.0 (CsOH) with an osmolality 300 mmol/kg. Barium currents were recorded in an extracellular solution containing (in mM) 80 Ba^{2+}, 160 Cl^-, and 5 HEPES, equilibrated to pH 7.35 (BaOH) and osmolality 297 mmol/kg (98.8 mM D-mannitol). To block L-type Ca^{2+} channels, extracellular solutions were replaced with the same solution additionally containing nifedipine (1 μM, 1:10,000 ethanol:water) and/or $CdCl_2$ (30 μM). Mibefradil (2.7 μM) was used to block 50% of L-type Ca^{2+} and 90% of T-type Ca^{2+} channel current [28]. Chemicals and drugs were purchased from Sigma-Aldrich Co. (St. Louis, MO).

Data analysis

Patch clamp data were analyzed using Clampfit (MDS Inc, Union City, CA) and SigmaPlot (SPSS Inc, Chicago, IL).

RESULTS

The presence of mRNA for the T-type Ca channel α subunits, α_{1G}, α_{1H} and α_{1I} was investigated by reverse transcription and PCR of total RNA derived from the external muscle layers of adult mouse jejunum. Total RNA purified from mouse hippocampus was used to provide a positive control for the effectiveness of the primers. α_{1G}, and α_{1H} mRNA was amplified from the jejunum but although α_{1I} transcripts were detected in the hippocampal samples, this was not detected in samples from jejunum (Fig 1a). The identity of the products was confirmed by sequencing of the excised, purified products. We used the same primers to test whether any of the transcripts were specifically expressed in cells from the circular smooth muscle layers of the gastric fundus and jejunum by isolating cells using laser capture micro-dissection. α_{1H} mRNA was amplified from all of the samples containing cells collected from the jejunum but the primers for α_{1G} and α_{1I} did not amplify products of the expected size in any of the jejunal LCM samples (Fig 1b).α_{1H} mRNA but not α_{1I} mRNA was also detected in cells collected from the circular muscle layer of the gastric fundus. The presence of α_{1G} mRNA in circular smooth muscle from the gastric fundus was indicated by a faint band in one of the four gastric fundus samples (Fig 1b). PCR amplification from single cells was used to further determine whether α_{1H} mRNA could be detected in smooth muscle cells identified by their spindle shape and in ICC identified by Kit immunoreactivity. A product that was confirmed by sequencing to be amplified from α_{1H} mRNA was detected in all of the tubes (n = 5 tubes) that contained either smooth muscle cells or Kit-positive ICC

(examples shown in Fig 1c). c-Kit mRNA was amplified from tubes containing Kit immunoreactive cells but was not amplified from tubes containing Kit-negative, spindle shaped cells (Fig 1c) confirming the identity of the collected cells. Representative PCR results are shown for a sample containing Kit-positive cells (S1) and Kit-negative cells (S2) as well as results from a separate RT-PCR reaction using Kit-positive cells (S3) and bath solution. A product was not amplified from a tube containing the bath water.

The presence of α_{1H} transcripts in cells from mouse jejunum smooth muscle suggested that cells from this region may express mibefradil-sensitive, nifedipine and Cd^{2+}- resistant T-type Ca^{2+} channels. To verify this, we did whole cell voltage clamp recordings on freshly dissociated myocytes from the mouse jejunum (Fig 2). In the presence of 1 μM nifedipine and 80 mM Ba^{2+}, an inward current was recorded that was inhibited by >90% with 2.7 μM mibefradil (Fig 2a). This rapidly inactivating current activated at −50 mV with a peak inward current at −5 mV (Fig 2aii). Cadmium (30 μM), expected to block L-type but not T-type Ca^{2+} channels, did not block the current and this Cd^{2+}-resistant current was also inhibited by more than 90% with 2.7 μM mibefradil (Fig 2b).

The molecular and functional evidence for T-type Ca^{2+} channels in the mouse jejunum prompted us to investigate whether inhibitors of T-type Ca^{2+} channels would affect the electrical slow wave in mouse jejunum. When studying balb/c wild type mice, mibefradil, at a concentration that will predominantly block T-type Ca^{2+} channels (2 μM, [28]), did not completely block the slow wave. However, the time constant for the rising phase of the electrical slow wave was increased from 0.093 ± 0.005 sec (n = 9 cells from 5 mice) to 0.171 ± 0.015 sec (n = 10 cells from 3 mice, $p < 0.01$) and the frequency of electrical slow waves was reduced from 0.67 ± 0.02 Hz to 0.59 ± 0.02 ($p < 0.05$). Mibefradil had no significant effect on the resting membrane potential of the impaled smooth muscle cells (−64.7 ± 2.9 mV in control, −69.2 ± 2.6 mV in mibefradil, P = 0.26) (Fig 3).

To further examine the contribution of α_{1H} T-type Ca^{2+} channel subunits on gastrointestinal smooth muscle function, we attempted to knock out expression of the functional protein by targeting the gene for α_{1H}, *cacna1h*. The targeting vector was designed to disrupt exons 3 to 6 of the genomic sequence as shown in Fig 4a. This region corresponds to amino acid residues 138 to 373 in the expressed protein. Southern analysis of genomic DNA obtained from tails of heterozygous animals and digested using EcoRI detected an 11 kb wildtype band and a 9.5 kb targeted band when using the external probe XP1, as shown in Fig 4b. Examples of Southern blots from wild type and heterozygous mice are shown in Fig 4b. Genotyping was also done by PCR using the primers JLR5 and JLR6 to identify the wild type allele and Puro3a and KO37 to identify the knockout allele. Mice heterozygous for the knockout allele survived, had no obvious phenotype and had no problems with breeding. However only one mouse homozygous for the knockout allele was identified by either PCR or Southern blot as shown in Table 1 (see also Fig 4b for examples).

In total more than 200 adult mice were tested for genotype without identifying a homozygous knockout animal, so we examined the proportions of the alleles in mice generated from ten separate pairs of heterozygous animals. The proportions of the genotypes of the mice obtained from breeding heterozygotes (Table 1), significantly deviated from the proportions predicted by Hardy Weinberg principles ($p < 0.0001$, χ^2 test) indicating that the homozygous knockout animals were dying prior to genotyping. We saw no evidence of pups dying shortly after birth. Therefore, we reasoned that the homozygous mutant animals were dying *in utero*. We tested whether the homozygous knockouts were dying before birth by mating 4 heterozygous pairs of mice. The females were killed at fixed times from the detection of vaginal plugs and the foetuses removed under sterile conditions. The foetuses were photographed and then tissue from the head was removed for DNA extraction and

genotyping. The proportions of the genotypes deviated significantly from Hardy Weinberg proportions ($p = 0.0015$, χ^2 test) and no foetuses homozygous for the mutated allele were detected in female mice more than 10.5 days after the plug was detected (see Table 1). However foetuses homozygous for the knockout allele were detected before embryonic day 10.5 in numbers that did not deviate significantly from Hardy Weinberg proportions ($p > 0.05$, χ^2 test, Table 1). The foetuses did not have anatomical abnormalities that allowed us to distinguish between knockout and heterozygous or wild type animals at embryonic age 9.5 to 10.5 (see Fig 5). The hearts were beating when the foetuses were removed and there were no clear neural tube defects. However, later during gestation (E17.5 to E19.5) reabsorbed foetuses were observed in the uteruses removed for genotyping of the foetuses.

We were unable to obtain more than one mouse that was homozygous for the knockout allele so we compared the properties of the electrical slow wave in the circular smooth muscle layer from the jejunum of 4 mice heterozygous for the knockout with the properties in 4 wild type siblings. 41 cells from heterozygous mutant mice and 39 cells from wild type mice were studied and no differences were detected in the rate of rise of the electrical slow wave as (Time constant in heterozygous animals = 0.143 ± 0.007 sec, homozygous wild type = 0.139 ± 0.006 sec, $P > 0.05$). The electrical slow wave recorded from smooth muscle cells in the jejunum in the one mouse homozygous for knockout of the α_{1H} gene appeared abnormal. The slope of the initial rising phase of the slow wave was lower than usual and the frequency of the slow waves was less than half the normal value (0.296 ± 0.009 Hz, n = 7 cells, Fig 6 vs 0.67 ± 0.02 Hz in 9 cells from 5 balb/c wild type mice, see above) with no clear difference in the resting membrane potential of the cells (−56.1 ± 2.3 mV, n = 7 cells vs −64.7 ± 2.9 mV in 9 cells from 5 balb/c wild type mice, see above).

DISCUSSION

Inward cationic conductances that are activated at comparatively negative membrane potentials (<−30 mV) and that are not selectively permeable, or are permeable to Ca^{2+} or Na^+, have been demonstrated in gastrointestinal smooth muscle cells and interstitial cells of Cajal from many species [3–9,24,29]. Due to recent pharmacological and technical advances, the biophysical and molecular identification of these conductances should be possible but so far few have been definitively identified [24]. In this study, we have demonstrated the expression of the α_{1H} Ca^{2+} channel subunit in the circular smooth muscle layer of the mouse jejunum and fundus, specifically in myocytes and ICC from the jejunum. We have also determined that inhibition of T-type Ca^{2+} currents affects the electrical slow wave in this tissue. We did not directly record from identified ICC in this manuscript and attempts to directly determine the contribution of the α_{1H} subunit to gastrointestinal function were not successful due to the lethal effects of knocking out the *cacna1h* gene, which encodes this protein.

The problems with dissecting out Ca^{2+} currents in myocytes and ICC are that some of the T-type Ca^{2+} channels are quite resistant to the effect of Ni^{2+} (>200 μM for α_{1I} and α_{1G}, [30]) and Ni^{2+} has effects on other Ca^{2+} permeable channels or transporters in the plasma membrane [31–34]. When used at the correct concentration, mibefradil is a fairly selective inhibitor of T-type Ca^{2+} channels [35] with a 4–10 fold higher potency as an inhibitor of T-type Ca^{2+} channels when compared to its effects on L-type Ca^{2+} channels and the sodium channel, $Na_v1.5$ [28] but it is often tested at concentrations that are not selective and its effects are diminished at positive membrane voltages [36]. Similarly, excluding the other Ca^{2+} permeable conductances in the cells can be difficult due to the lack of selective inhibitors of non-selective cation conductances. When L-type Ca^{2+} currents are present in the cells, these currents can be inhibited by dihydropyridine calcium channel blockers but the effectiveness of dihydropyridines is reduced at the more negative membrane voltages

[37] where the low voltage activated current is observed, possibly leading to the erroneous identification of residual L-type current as a low voltage activated Ca^{2+} current. In addition dihydropyridines inhibit some T-type Ca^{2+} channels at concentrations greater than 5 μM [38].

The molecular identification of the α_{1H} subunit in mouse jejunal smooth muscle is consistent with the biophysical and pharmacological properties of the low voltage activated Ca^{2+} selective conductance reported herein in mouse jejunal myocytes and recorded by several groups in smooth muscle cells from rat small intestine [3] as well as myocytes from other gastrointestinal tissue [3,6–9]. Specifically, the α_{1H} Ca^{2+} channel subunit is resistant to inhibition by nifedipine and Cd^{2+} and is blocked by mibefradil at 2.7 μM [35]. Other distinguishing properties of the α_{1H} Ca^{2+} channel subunit are activation starting at −60 mV and similar relative selectivity and permeability to Ca^{2+} and Ba^{2+} ions.

None of the previously published studies on the expression of T-type Ca^{2+} channel α subunits have tested for the presence of the α_{1H} subunit and none have identified a candidate for the low voltage activated cation conductance in myocytes from rodent circular smooth muscle [5,23]. In one study, mRNA for the α_{1G} subunit was not detected in myocytes from mouse colonic circular muscle [5]. In the other study, the presence was demonstrated of all three T-type Ca^{2+} channel α subunits in the external muscle layers of mouse small intestine but this study did not determine if myocytes expressed the mRNA for any of the subunits. We could not detect the α_{1I} subunit mRNA in our samples even though the primers worked in our positive control experiment. Three different primer sets were tested for the α_{1I} subunit and none amplified a product of the expected size (data not shown). One possible explanation for the amplification of α_{1H} Ca^{2+} channel mRNA from the circular smooth muscle layer of the mouse jejunum is that the mRNA came from a cell type other than the myocytes or ICC. In human myometrium, α_{1H} Ca^{2+} channel immunoreactivity was detected in lymphocytes but not smooth muscle cells [1]. This is consistent with a role for T-type Ca^{2+} channels in the migration of leucocytes [39]. However, the samples that we collected by laser capture microdissection were from histochemically stained sections and were taken from the circular smooth muscle layer in regions that did not show evidence of lymphocytic contamination. In addition, the single cells that we collected were either Kit-immunoreactive or had myocyte morphology, so we consider it unlikely that this could account for the results.

The reduction in the rate of rise of the electrical slow wave recorded in myocytes of mouse jejunum in response to mibefradil treatment is consistent with an effect of mibefradil on ICC as previously published in other tissues. The upstroke of electrical slow waves recorded in mouse small intestine involves Ca^{2+} influx through a non-L type Ca^{2+} channel [15], Ni^{2+} (1 – 100 μM) reduces the rate of rise of slow waves in guinea pig gastric antrum [40] and the upstroke of pacemaker potentials in mouse ICC recorded by Ca^{2+} imaging was inhibited by mibefradil (0.1 μM) and Ni^{2+} (100 μM) [20]. These experimental results are further supported by mathematical models of pacemaker potentials in ICC that show the necessity for a voltage activated Ca^{2+} current in order to accurately model the pacemaker potentials. [41]. Interestingly, slowing of the rise time for the electrical slow wave in mice in mibefradil and Ni^{2+} is similar to the effects of inhibiting the tetrodotoxin (TTX) -resistant Na^{+} channel, $Na_v1.5$ on the electrical slow wave recorded in circular muscle of human jejunum [29]. Also, mibefradil and Ni^{2+} do not completely block the upstroke at concentrations where near complete inhibition of a T-type channel is expected [18] suggesting the possibility that more than one channel type may contribute to the upstroke. These pharmacological properties also raise the possibility that the observed current carried by non-L-type Ca^{2+} channels is carried by T-type-like channels and the possibility that the current is carried by a combination of alpha subunits or a novel T-type alpha subunit cannot be excluded.

The target for mibefradil is likely the α_{1H} channel subunit identified in ICC by single cell PCR rather than in smooth muscle because the electrical slow wave is generated by ICC in the myenteric plexus region of the mouse jejunum, where the pacemaker potential is initiated. As the slow wave is generated by ICC, there should not be a need for a T-type Ca^{2+} channel to participate in the generation of the upstroke in smooth muscle cells. It may be that Ca^{2+} influx through T-type Ca^{2+} channels in myocytes is more important for functions of Ca^{2+} unrelated to contractility such as cellular proliferation or migration. In this respect, myocytes from mouse jejunum are similar to other smooth muscles [2,42] although there does appear to be role for α_{1H} Ca^{2+} channel subunits in controlling relaxation of coronary smooth muscle [43].

Studies in the mice heterozygous for the knockout of the α_{1H} Ca^{2+} channel subunit did not provide any further information because when compared with wild type litter-mates, there were no differences in the properties of the electrical slow wave. This indicates that the partial knockout did not have a gene dosing effect.

The lethal effects of knocking out expression of the α_{1H} Ca^{2+} channel subunit in all but one of the many hundreds of mice studied were surprising given that another group has successfully generated a strain of mice by deletion of exon 6 in the *cacna1h* gene [43]. The reported effects of this knockout were cardiac injury due to coronary artery constriction and reduced body mass compared to wild type litter mates. These are both phenotypes consistent with reduced survival but were clearly not sufficient to prevent survival to maturity of the knockout mice [43]. We were only able to obtain one adult mouse homozygous for the knockout allele over a period of 4 years studying these animals and we conclude that this very low survival rate reflects the genetic backgrounds of the strain of either embryonic stem cells or recipient blastocysts [44]. We could not identify the actual cause of death of the homozygous knockout foetuses but death of foetuses at ages around E10.5 is associated with cardiovascular abnormalities (e.g. [45] and this is consistent with both the phenotype of the published α_{1H} knockout [43] and the known role of T-type Ca^{2+} channels in smooth muscle cell growth and proliferation [2]. Neural tube abnormalities, which also can cause embryonic lethality at around E10.5 [46], were not observed. Interestingly, the rate of rise and frequency of the electrical slow wave were lower than normal values in recordings from the jejunum of the one mouse that did survive.

In conclusion, the α_{1H} Ca^{2+} channel subunit is expressed in myocytes and ICC from the circular muscle layer of mouse jejunum. A T-type Ca^{2+} current also appears to play a role in the generation of the upstroke of the electrical slow wave in mouse tissue and the pharmacological properties of this current are consistent with expression of the α_{1H} Ca^{2+} channel subunit in ICC contributing to this current. The phenotypic effect of knocking out the gene for the α_{1H} Ca^{2+} channel subunit is dependent the genetic background of the mouse strain used for the construct and can be embryonic lethal in some mouse strains.

Acknowledgments

We thank Dr Stephen Thibodeau (and his lab) for his assistance with the Southern blots and Dr Jan Van Deursen (and his lab, especially Darren Baker) for their assistance with dissecting out the mouse embryos. This work was supported by the following grants from the NIH, DK 52766, DK 57061 and DK 68055.

References

1. Blanks AM, Zhao ZH, Shmygol A, Bru-Mercier G, Astle S, Thornton S. Characterization of the molecular and electrophysiological properties of the T-type calcium channel in human myometrium. J Physiol 2007;581:915–26. [PubMed: 17446221]

2. Cribbs LL. T-type Ca2+ channels in vascular smooth muscle: multiple functions. Cell Calcium 2006;40:221–30. [PubMed: 16797699]

3. Xiong Z, Sperelakis N, Noffsinger A, Fenoglio-Preiser C. Changes in calcium channel current densities in rat colonic smooth muscle cells during development and aging. Am J Physiol 1993;265:C617–25. [PubMed: 8214017]

4. Xiong Z, Sperelakis N, Noffsinger A, Fenoglio-Preiser C. Ca2+ currents in human colonic smooth muscle cells. Am J Physiol 1995;269:G378–85. [PubMed: 7573448]

5. Koh SD, Monaghan K, Ro S, Mason HS, Kenyon JL, Sanders KM. Novel voltage-dependent non-selective cation conductance in murine colonic myocytes. J Physiol 2001;533:341–55. [PubMed: 11389196]

6. Yamamoto Y, Hu SL, Kao CY. Inward current in single smooth muscle cells of the guinea pig taenia coli. J Gen Physiol 1989;93:521–50. [PubMed: 2539433]

7. Yoshino M, Someya T, Nishio A, Yazawa K, Usuki T, Yabu H. Multiple types of voltage-dependent Ca channels in mammalian intestinal smooth muscle cells. Pflugers Arch 1989;414:401–9. [PubMed: 2477791]

8. Lee HK, Sanders KM. Comparison of ionic currents from interstitial cells and smooth muscle cells of canine colon. J Physiol 1993;460:135–52. [PubMed: 8387582]

9. Kim YC, Koh SD, Sanders KM. Voltage-dependent inward currents of interstitial cells of Cajal from murine colon and small intestine. J Physiol 2002;541:797–810. [PubMed: 12068041]

10. Farrugia G. Interstitial cells of Cajal in health and disease. Neurogastroenterol Motil 2008;20:54–63. [PubMed: 18402642]

11. Huizinga JD, Thuneberg L, Kluppel M, Malysz J, Mikkelsen HB, Bernstein A. W/kit gene required for interstitial cells of Cajal and for intestinal pacemaker activity. Nature 1995;373:347–9. [PubMed: 7530333]

12. Ward SM, Burns AJ, Torihashi S, Sanders KM. Mutation of the proto-oncogene c-kit blocks development of interstitial cells and electrical rhythmicity in murine intestine. J Physiol 1994;480:91–7. [PubMed: 7853230]

13. Huizinga JD, Zhu Y, Ye J, Molleman A. High-conductance chloride channels generate pacemaker currents in interstitial cells of Cajal. Gastroenterology 2002;123:1627–36. [PubMed: 12404237]

14. Sanders KM, Koh SD, Ward SM. Interstitial cells of cajal as pacemakers in the gastrointestinal tract. Annu Rev Physiol 2006;68:307–43. [PubMed: 16460275]

15. Malysz J, Richardson D, Farraway L, Christen MO, Huizinga JD. Generation of slow wave type action potentials in the mouse small intestine involves a non-L-type calcium channel. Can J Physiol Pharmacol 1995;73:1502–11. [PubMed: 8748943]

16. Hotta A, Okada N, Suzuki H. Mibefradil-sensitive component involved in the plateau potential in submucosal interstitial cells of the murine proximal colon. Biochem Biophys Res Commun 2007;353:170–6. [PubMed: 17174936]

17. Yoneda S, Takano H, Takaki M, Suzuki H. Effects of nifedipine and nickel on plateau potentials generated in submucosal interstitial cells distributed in the mouse proximal colon. J Smooth Muscle Res 2003;39:55–65. [PubMed: 14572173]

18. Kito Y, Ward SM, Sanders KM. Pacemaker potentials generated by interstitial cells of Cajal in the murine intestine. Am J Physiol Cell Physiol 2005;288:C710–20. [PubMed: 15537708]

19. Lee HT, Hennig GW, Fleming NW, Keef KD, Spencer NJ, Ward SM, Sanders KM, Smith TK. The mechanism and spread of pacemaker activity through myenteric interstitial cells of Cajal in human small intestine. Gastroenterology 2007;132:1852–65. [PubMed: 17484879]

20. Park KJ, Hennig GW, Lee HT, Spencer NJ, Ward SM, Smith TK, Sanders KM. Spatial and temporal mapping of pacemaker activity in interstitial cells of Cajal in mouse ileum in situ. Am J Physiol Cell Physiol 2006;290:C1411–27. [PubMed: 16381798]

21. Farrugia G. Ca2+ handling in human interstitial cells of Cajal. Gastroenterology 2007;132:2057–9. [PubMed: 17484898]

22. Perez-Reyes E. Molecular characterization of T-type calcium channels. Cell Calcium 2006;40:89–96. [PubMed: 16759699]

23. Chen H, Redelman D, Ro S, Ward SM, Ordog T, Sanders KM. Selective labeling and isolation of functional classes of interstitial cells of Cajal of human and murine small intestine. Am J Physiol Cell Physiol 2007;292:C497–507. [PubMed: 16943245]
24. Ou Y, Gibbons SJ, Miller SM, Strege PR, Rich A, Distad MA, Ackerman MJ, Rae JL, Szurszewski JH, Farrugia G. SCN5A is expressed in human jejunal circular smooth muscle cells. Neurogastroenterol Motil 2002;14:477–86. [PubMed: 12358675]
25. Wouters MM, Gibbons SJ, Roeder JL, Distad M, Ou Y, Strege PR, Szurszewski JH, Farrugia G. Exogenous serotonin regulates proliferation of interstitial cells of Cajal in mouse jejunum through 5-HT2B receptors. Gastroenterology 2007;133:897–906. [PubMed: 17854596]
26. Farrugia G, Irons WA, Rae JL, Sarr MG, Szurszewski JH. Activation of whole cell currents in isolated human jejunal circular smooth muscle cells by carbon monoxide. Am J Physiol 1993;264:G1184–9. [PubMed: 8392811]
27. Farrugia G, Rae JL, Szurszewski JH. Characterization of an outward potassium current in canine jejunal circular smooth muscle and its activation by fenamates. J Physiol 1993;468:297–310. [PubMed: 8254511]
28. Strege PR, Bernard CE, Ou Y, Gibbons SJ, Farrugia G. Effect of mibefradil on sodium and calcium currents. Am J Physiol Gastrointest Liver Physiol 2005;289:G249–53. [PubMed: 15790762]
29. Strege PR, Ou Y, Sha L, Rich A, Gibbons SJ, Szurszewski JH, Sarr MG, Farrugia G. Sodium current in human intestinal interstitial cells of Cajal. Am J Physiol Gastrointest Liver Physiol 2003;285:G1111–21. [PubMed: 12893628]
30. Lee JH, Gomora JC, Cribbs LL, Perez-Reyes E. Nickel block of three cloned T-type calcium channels: low concentrations selectively block alpha1H. Biophys J 1999;77:3034–42. [PubMed: 10585925]
31. Chaib N, Kabre E, Metioui M, Alzola E, Dantinne C, Marino A, Dehaye JP. Differential sensitivity to nickel and SK&F96365 of second messenger-operated and receptor-operated calcium channels in rat submandibular ductal cells. Cell Calcium 1998;23:395–404. [PubMed: 9924631]
32. Hinde AK, Perchenet L, Hobai IA, Levi AJ, Hancox JC. Inhibition of Na/Ca exchange by external Ni in guinea-pig ventricular myocytes at 37 degrees C, dialysed internally with cAMP-free and cAMP-containing solutions. Cell Calcium 1999;25:321–31. [PubMed: 10456229]
33. Kimura J, Miyamae S, Noma A. Identification of sodium-calcium exchange current in single ventricular cells of guinea-pig. J Physiol 1987;384:199–222. [PubMed: 2443659]
34. Ng LC, Gurney AM. Store-operated channels mediate Ca(2+) influx and contraction in rat pulmonary artery. Circ Res 2001;89:923–9. [PubMed: 11701620]
35. Martin RL, Lee JH, Cribbs LL, Perez-Reyes E, Hanck DA. Mibefradil block of cloned T-type calcium channels. J Pharmacol Exp Ther 2000;295:302–8. [PubMed: 10991994]
36. Bezprozvanny I, Tsien RW. Voltage-dependent blockade of diverse types of voltage-gated Ca2+ channels expressed in Xenopus oocytes by the Ca2+ channel antagonist mibefradil (Ro 40-5967). Mol Pharmacol 1995;48:540–9. [PubMed: 7565636]
37. Bean BP. Nitrendipine block of cardiac calcium channels: high-affinity binding to the inactivated state. Proc Natl Acad Sci U S A 1984;81:6388–92. [PubMed: 6093100]
38. Shcheglovitov A, Zhelay T, Vitko Y, Osipenko V, Perez-Reyes E, Kostyuk P, Shuba Y. Contrasting the effects of nifedipine on subtypes of endogenous and recombinant T-type Ca2+ channels. Biochem Pharmacol 2005;69:841–54. [PubMed: 15710361]
39. Nebe B, Holzhausen C, Rychly J, Urbaszek W. Impaired mechanisms of leukocyte adhesion in vitro by the calcium channel antagonist mibefradil. Cardiovasc Drugs Ther 2002;16:183–93. [PubMed: 12374895]
40. Tomita T, Pang YW, Ogino K. The effects of nickel and cobalt ions on the spontaneous electrical activity, slow wave, in the circular muscle of the guinea-pig gastric antrum. J Smooth Muscle Res 1998;34:89–100. [PubMed: 9972518]
41. Faville RA, Pullan AJ, Sanders KM, Smith NP. A biophysically based mathematical model of unitary potential activity in interstitial cells of Cajal. Biophys J 2008;95:88–104. [PubMed: 18339738]

42. Fry CH, Sui G, Wu C. T-type Ca2+ channels in non-vascular smooth muscles. Cell Calcium 2006;40:231–9. [PubMed: 16797698]

43. Chen CC, Lamping KG, Nuno DW, Barresi R, Prouty SJ, Lavoie JL, Cribbs LL, England SK, Sigmund CD, Weiss RM, Williamson RA, Hill JA, Campbell KP. Abnormal coronary function in mice deficient in alpha1H T-type Ca2+ channels. Science 2003;302:1416–8. [PubMed: 14631046]

44. Gerlai R. Gene-targeting studies of mammalian behavior: is it the mutation or the background genotype? Trends Neurosci 1996;19:177–81. [PubMed: 8723200]

45. Takeshima H, Komazaki S, Hirose K, Nishi M, Noda T, Iino M. Embryonic lethality and abnormal cardiac myocytes in mice lacking ryanodine receptor type 2. Embo J 1998;17:3309–16. [PubMed: 9628868]

46. Harris MJ, Juriloff DM. Mini-review: toward understanding mechanisms of genetic neural tube defects in mice. Teratology 1999;60:292–305. [PubMed: 10525207]

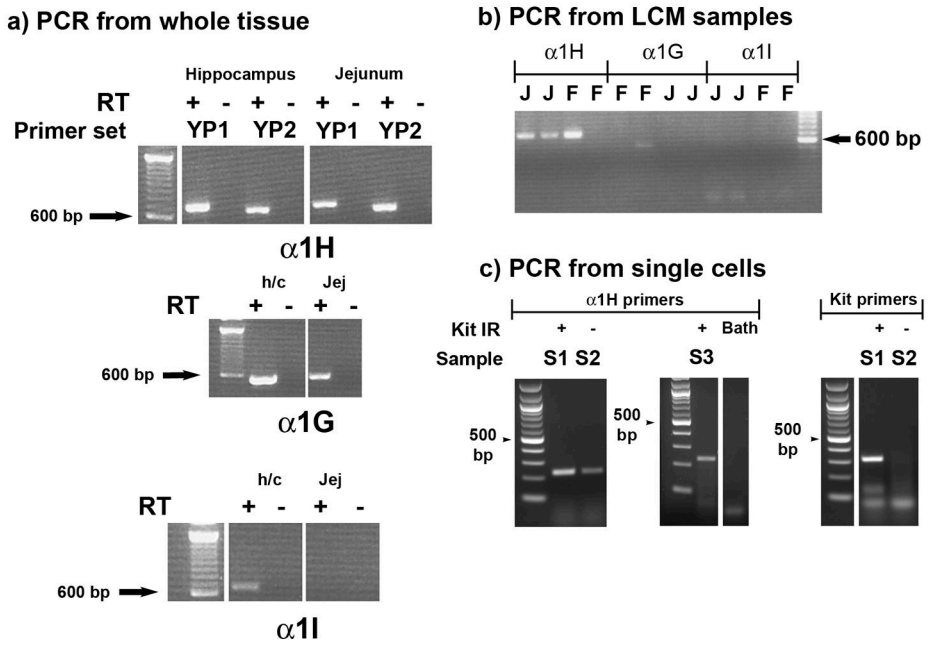

Figure 1.

a) PCR amplification of T-type Ca^{2+} channel α subunit mRNA from the external muscle layers of adult mouse jejunum. Amplification from hippocampal mRNA is shown as a positive control. YP1 and YP2 represent two different primer sets (see Table 1 for details). b) PCR amplification of T-type Ca^{2+} channel α subunit mRNA from smooth muscle cells from wild type (WT) mouse jejunum and fundus that were collected by laser capture micro-dissection (LCM). C) Representative PCR amplifications of T-type Ca^{2+} channel α subunit mRNA from single tubes of Kit immunoreactive (Kit-IR, S1 and S3) and Kit-negative spindle-shaped cells (S2). A sample of the bath solution (BATH) was also collected and subjected to RT-PCR as a negative control. Primers were designed against the T-type Ca^{2+} channel subunit covering at least one intron to avoid genomic contamination. The specific products for α_{1H} were amplified by reverse transcription PCR (RT-PCR). J = jejunum; F = fundus, RT –, control for genomic contamination i.e. underwent RT-PCR in the absence of reverse transcriptase. A 100bp DNA ladder was loaded and is shown to indicate product size.

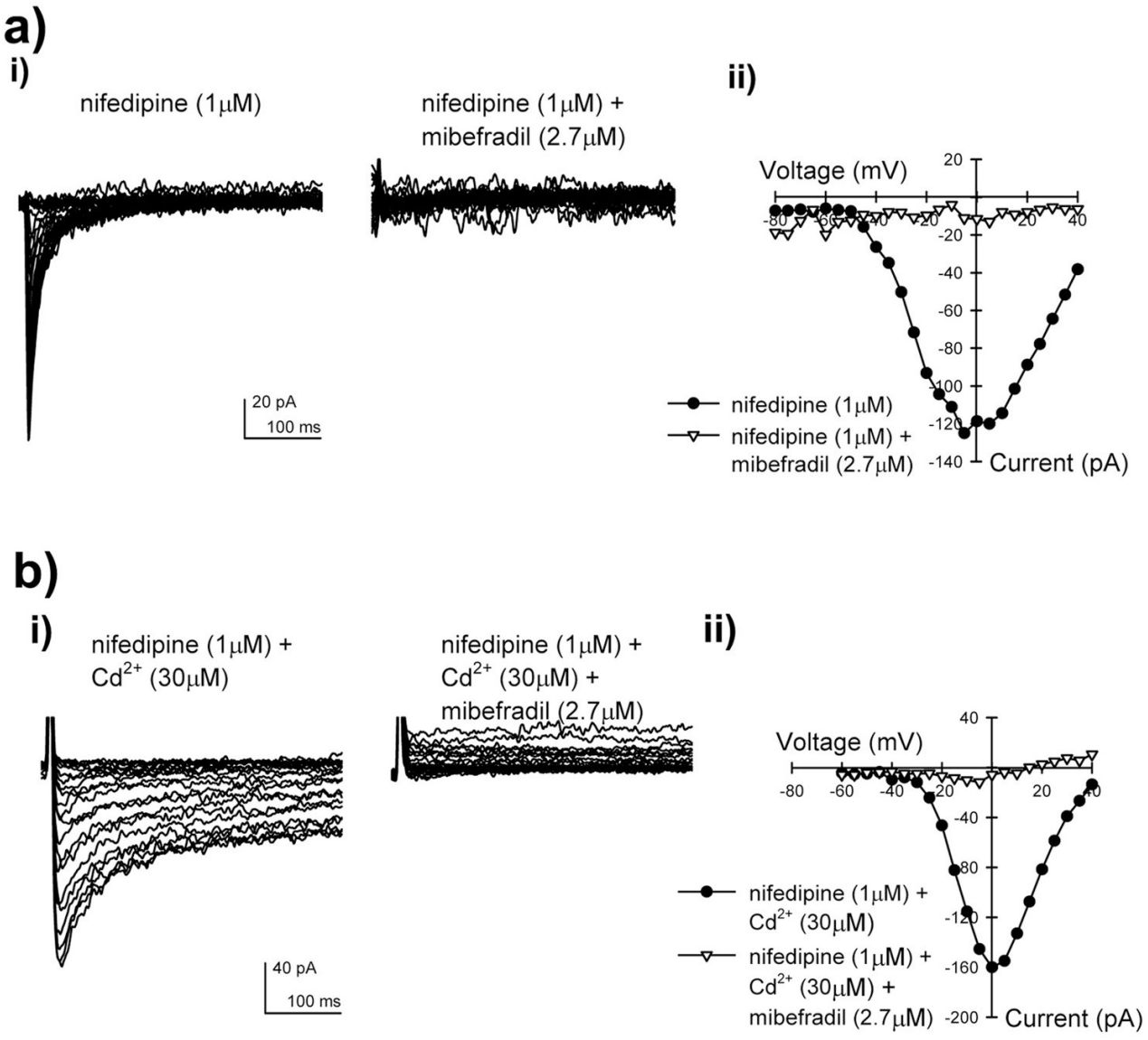

Figure 2.

Representative T-type whole cell currents recorded in myocytes from the outer muscle layers of the mouse jejunum. a) i) Nifedipine-resistant, mibefradil-sensitive Ba^{2+} currents, ii) Current-voltage relationship for the peak inward currents show in (a)i. b) i) Mibefradil-sensitive Ba^{2+} currents obtained in the presence of nifedipine and Cd^{2+}, ii) Current-voltage relationship for the peak inward currents shown in (b)i. Currents were recorded by stepping the command voltage from −100 mV to between −80 to +35 mV in 5 mV steps.

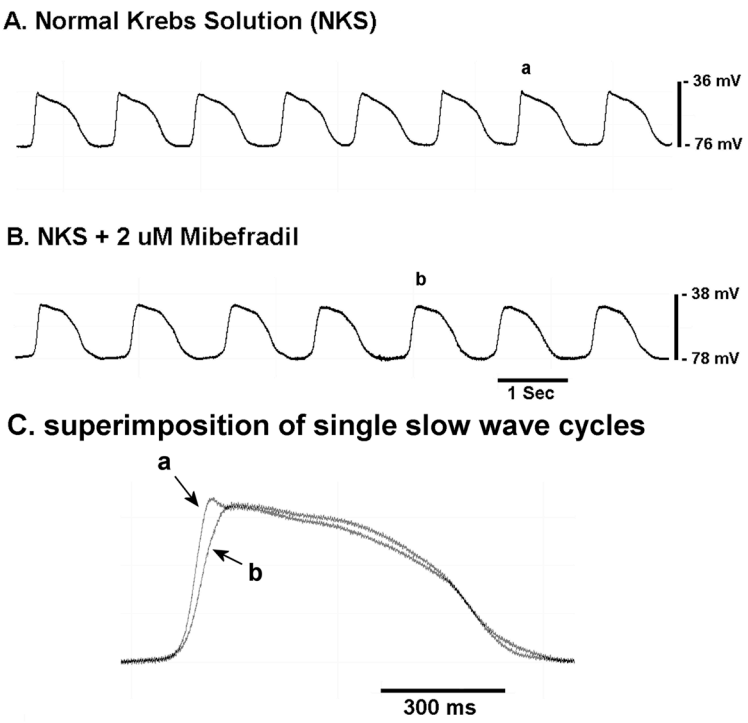

Figure 3.

Mibefradil reduces the initial rate of rise and frequency of the electrical slow wave in the circular smooth muscle layer of the mouse jejunum.

a) Control recording, b) recording in the presence of 2 μM mibefradil c) superimposition of single slow wave cycles to show the effect of mibefradil.

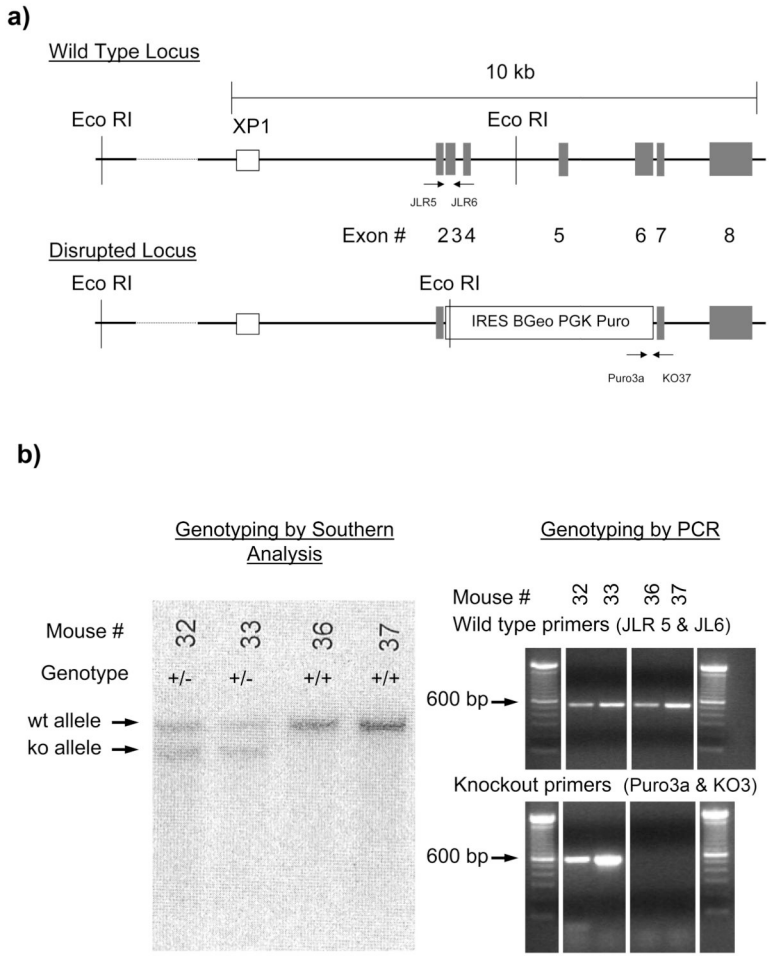

Figure 4.

Gene targeted knockout of the α_{1H} Ca^{2+} channel subunit in mice.

a) Schematic of the wild type and disrupted alleles showing the distribution of exons 2 to 8, the location of the key EcoR1 restriction sites for Southern blot analysis. The location of the binding sites for the Southern blot probe (XP1) and the oligonucleotide PCR primers for identifying the wild type (JLR5 and JLR6) and disrupted (Puro3a and KO37) alleles are also shown. A 100bp DNA ladder was loaded and is shown to indicate product size.

b) Example of Southern blot analysis of the alleles present in the genomes of 4 mice is shown together with PCR confirmation of the genotype using DNA samples from the same mice.

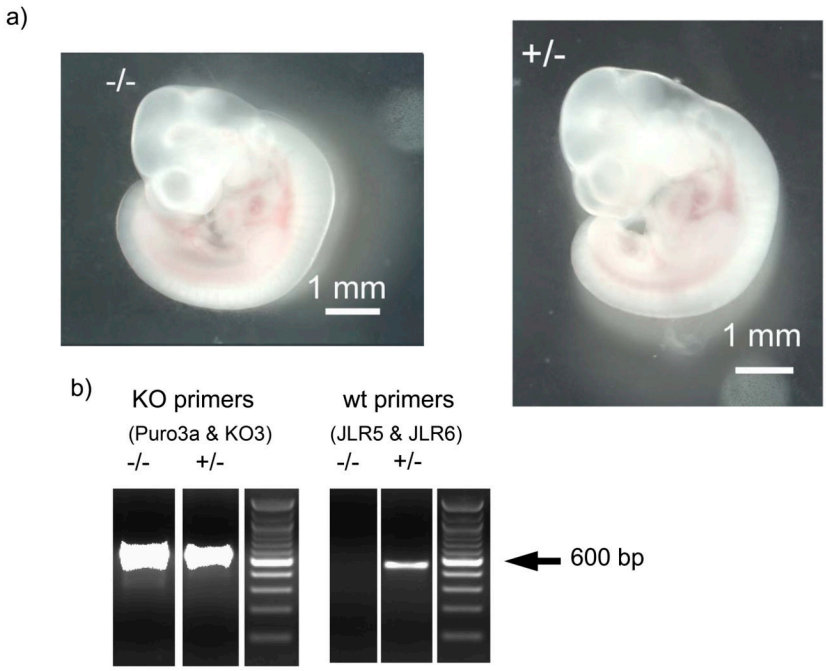

Figure 5.

Foetuses homozygous or heterozygous for the knockout of the *cacna1h* gene exhibit no gross abnormalities. a) Images of foetuses obtained 9 days after detection of a vaginal plug (E9.5). b) Results of PCR genotyping of the foetuses shown. (KO – knockout, wt - wild type). A 100bp DNA ladder was loaded and is shown to indicate product size.

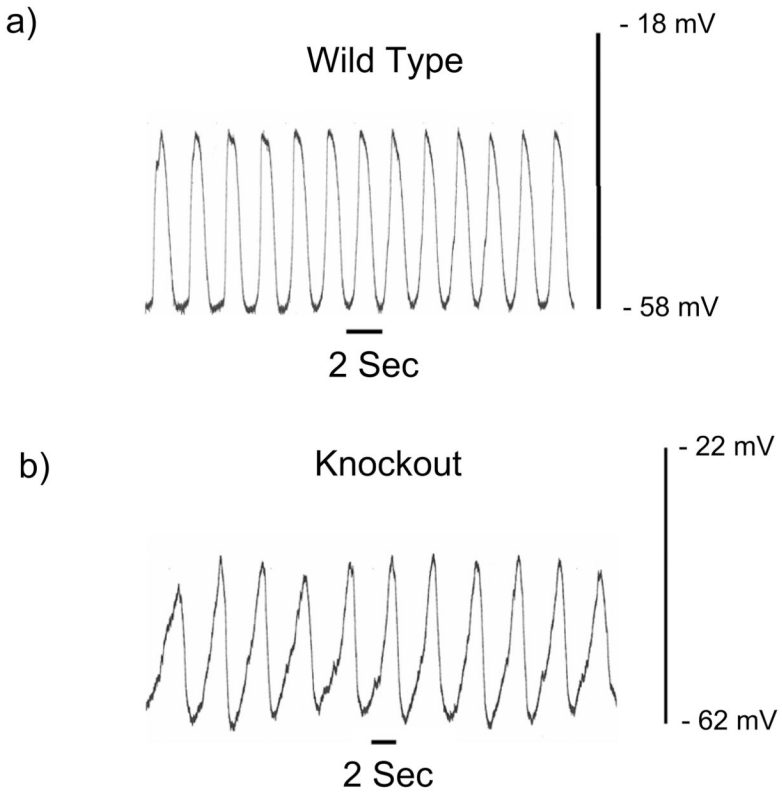

Figure 6.

The initial rate of rise and frequency of the electrical slow wave recorded in the circular smooth muscle layer of the mouse jejunum are lower in a mouse homozygous for the α_{1H} knockout.

a) Control recording from a wild type balb/c mouse, b) Recording from a homozygous knockout mouse.

TABLE 1

Target (Primer Name)	Forward Primer	Reverse Primer	Expected size (bp)
PCR Primers			
Alpha 1H (YP1)	GCATGGCCTTCCTCACGTTGTT	GTGTAGTCTGGGATGCCGTCTT	697
(YP2)	TGCCGGTGGTGCCAAGATCCTA	GGCGCGTGTGTGAATAGTCTGC	628
Alpha 1G	CTACGGTCCCTTCGGCTACATT	TCCACTCGTATCTTCCCGTTTG	531
Alpha 1I	CTGTTTAGTCTGCGTGGGCTG	CTAACCCAGACCCTCTCAGTC	608
Single Cell PCR Primers			
Alpha 1H (Outer)	CTTCTTGCGGCCATACTACC	CTGGTTTTCCCTCTGCTTTG	475
Alpha 1H (Inner)	TCACAATGGTGCCATCAACT	CTGGTTTTCCCTCTGCTTTG	232
Kit (Outer)	ATTATGAACGCCAGGAGACG	GAATCCCTCTGCCACACACT	497
Kit (Inner)	TACGAGGCCTACCCCAAACC	CTCTGCCACACACTGGAGCA	285
Genotyping Primers			
Wild Type	AGGAGAGGCACTTACTGG	TAGGTATCAAGGACTGTGAGG	487
Knockout	CGCAAGCCCGGTGCCTGA	CCCTGTCCTGAGTAGAACTG	520

TABLE 2

Genotypes of mice resulting from mating of pairs of heterozygous animals

	Post-natal	Embryonic Age E17.5 to E19.5	Embryonic Age E9.5 to E10.5
Wild Type	26 (33%)	3 (16%)	2 (10%)
Heterozygous	54 (66%)	16 (84%)	10 (47%)
Homozygous Knockout	1 (1%)	0 (0%)	9 (43%)
No. Litters	**10**	**2**	**2**